Biophysical Chemistry 162 (2012) 35–44

Contents lists available at SciVerse ScienceDirect

Biophysical Chemistry

journal homepage: http://www.elsevier.com/locate/biophyschem

Molecular dynamics simulations for glutamate-binding and cleft-closing processes of the ligand-binding domain of GluR2

Okimasa Okada [a,*], Kei Odai [b], Tohru Sugimoto [c], Etsuro Ito [d]

[a] ZoeGene Corporation, Yokohama, Kanagawa 227–0033, Japan
[b] Department of Informatics and Media Technology, Shohoku College, Astugi, Kanagawa 243–8501, Japan
[c] Department of Humanities, College of Engineering, Kanto Gakuin University, Yokohama, Kanagawa 236-8501, Japan
[d] Kagawa School of Pharmaceutical Sciences, Tokushima Bunri University, Sanuki, Kagawa 769-2193, Japan

HIGHLIGHTS

- Unbiased MD simulations reveal the spontaneous glutamate-binding and cleft-closing mechanisms.
- The glutamate is attracted by ARG485 to enter the cleft from a more flexible side without the S–S bond.
- The orientation of the glutamate upon binding is regulated by TYR450 with the cation–π interaction.
- A semi-open state is identified in the free energy profile obtained by the unbiased MD simulations.
- The so-called linear response theory is verified in the inter-domain motion of the LBD of GluR2.

GRAPHICAL ABSTRACT

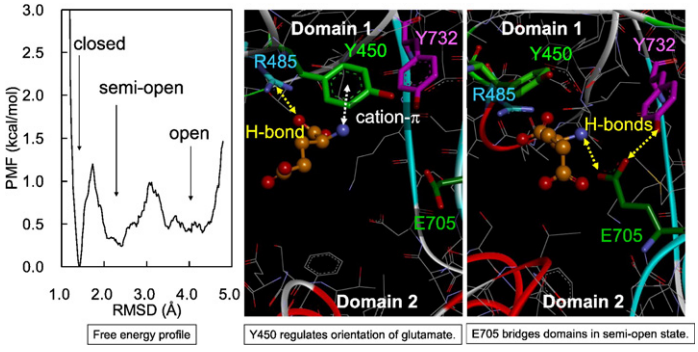

ARTICLE INFO

Article history:
Received 23 October 2011
Received in revised form 12 December 2011
Accepted 20 December 2011
Available online 28 December 2011

Keywords:
Unbiased molecular dynamics simulation
Free energy profile
Semi-open state
Inter-domain conformational change
Glutamate binding pathway

ABSTRACT

The gating of ion channel of ionotropic glutamate receptors is controlled by the structural change of the ligand-binding domain of GluR2. We examined the roles of residues in the glutamate-binding and cleft-closing mechanisms by molecular dynamics (MD) simulations. A glutamate entered the cleft deeply within the order of nanoseconds and the cleft locked the glutamate completely at 15 ns in an MD run. TYR450 seemed to regulate the orientation of the glutamate upon binding by cation–π interaction. A semi-open state was identified in the free energy profile evaluated with the structures on the spontaneously glutamate-bound and cleft-closed pathway by the unbiased MD simulations for the first time to our knowledge. In the semi-open state, the two sub-domains were bridged by two hydrogen bonds of GLU705 in the sub-domain 2 with TYR732 in the sub-domain 1 and with the glutamate bound to the sub-domain 1 until the transition to the closed state.

1. Introduction

The ionotropic glutamate receptors (iGluRs) are categorized into three subclasses by their agonists, which are α-amino-3-hydroxy-5-methyl-4-isoxazole propionic acid (AMPA; GluR1-4), kainate (KA; GluR5-7 and KA1-2), and *N*-methyl-D-aspartate (NMDA; NR1-3) [1,2]. The iGluR is composed of one transmembrane domain and

* Corresponding author at: Mitsubishi Tanabe Pharma Corporation, Medicinal Chemistry Research Laboratories II, 2-2-50, Kawagishi, Toda-shi, Saitama 335-8505, Japan. Tel.: +81 48 433 8031; fax: +81 48 433 2849.
E-mail address: Okada.Okimasa@mc.mt-pharma.co.jp (O. Okada).

0301-4622/$ – see front matter © 2011 Elsevier B.V. All rights reserved.
doi:10.1016/j.bpc.2011.12.004

two extracellular domains, i.e., a ligand-binding domain (LBD) and an amino-terminal domain (ATD). Four subunits of iGluRs are arranged in a dimer of dimers form constructing an ion-channel pore at their central region, and they are responsible for a large portion of the fast excitatory neurotransmission in the mammalian brain [3–6]. The glutamate receptor subunit 2 (GluR2) is one of the subfamilies of iGluRs, and it is thought to play important roles in gating the ion channel and restraining the flow of Ca^{2+} [7–9].

The co-crystal structure of the LBD of GluR2 with kainate was first solved by Armstrong et al. in 1998 [10]. The co-crystal structures of the LBDs with the full agonists, partial agonists, and antagonists have also been solved by X-ray analyses [11–17]. More recently, the structure of the GluR2, including the transmembrane domain, LBD, and ATD, has been analyzed by Sovolevsky et al [6]. They showed that the extracellular domains have a two-fold symmetry and that the transmembrane domain has a four-fold symmetry. They also proposed that the closure of LBD (i.e., the cleft) by the agonist binding resulted in an increase in the separation of the transmembrane domain linkers and activation of the opening of the ion channel. The desensitization is thought to take place by rupture of the interface between two sub-domains (D1–D1) in the dimer with the agonist in the LBD.

The gating mechanism of the ion channel of GluR2 has been proposed by comparing the crystal structure of the apo state with the co-crystal structures with its full agonists (glutamate and AMPA), a partial agonist (kainate), and an antagonist (DNQX: 6,7-dinitro-2,3-quinoxzlinedione) [11]. When the agonist binds to the LBD, its structure is changed from the apo open state to the closed state by the interaction with the residues and water molecules in the cleft as well as by the interaction through the inter-domain hydrogen bonds. This structural change induces the rearrangement of four iGluR subunits in order to open the ion-channel pore. On the other hand, even if the antagonist binds to the LBD, its structure remains in the open state and so the ion channel cannot be opened.

The glutamate-binding process in the LBD was roughly proposed by using the X-ray crystal structures as follows [11]. First, the glutamate binds to the residues (ARG485, THR480, and PRO478 in the sub-domain 1 (D1), and GLU705 in the sub-domain 2 (D2)). Then, the closure of the cleft occurs by the interaction of the gamma carboxyl group of the glutamate with the base of the helix F of D2 and water molecules. It is inferred that the glutamate first binds to the binding site in the D1 quickly, and then the cleft closes slowly, suggesting that this closing step leads to the ion channel activation. The binding of the glutamate to close the cleft is expected to be a stochastic process, but it is almost impossible to obtain a detailed trace of the position of the glutamate upon binding by means of experiments. The molecular dynamics (MD) simulations for the LBDs of GluR2 [18–26] as well as other glutamate receptors [27,28] have been performed mostly to investigate the gating mechanism of the ion channels by the structural changes of receptors. However, these simulations, which were focused only on the structural changes of the LBD, did not deal with the glutamate-binding and cleft-closing processes.

On the other hand, as for other receptors, there have been theoretical studies investigating the ligand-binding processes. Binding MD simulations have been performed to clarify the binding of an aspartate into its racemase from the hyperthermophilic archaeon *Pyrococcus horikoshii* OT3, and the simulations predicted the entry process to the active site [29]. The formation process of a stable complex of a palmitate with a fatty acid-binding protein was also predicted using MD simulations [30]. More recently, the pathway and the mechanism of a drug binding to G-protein-coupled receptors were clarified by the unbiased MD simulations [31].

In these studies, the proteins and ligands formed the complexes spontaneously, though a huge amount of computation is required to observe a rare binding event in the MD simulations. The roles of several residues at the pocket upon ligand binding could be speculated by comparing the simulation results and the experimental results. Thus, we believe that the unbiased binding simulation, which uses no artificial external force, is a powerful tool to investigate the molecular recognition at the atomic level to complement the experimental data.

In the present study, we performed the MD calculations, without applying any artificial external forces, to elucidate the binding process of the glutamate into the LBD of GluR2 and that of the cleft-closing mechanism, and thereby to clarify the roles of residues of the cleft of GluR2 in the glutamate-binding and cleft-closing processes.

2. Materials and methods

2.1. Model preparation

The crystal structure of the LBD of GluR2 in the apo state (PDB: 1FTO) was obtained from the Protein Data Bank (PDB, http://www.rcsb.org). We chose the chain-A in the PDB data to use for our MD simulations (Fig. 1). The residue numbers we used correspond to those used by Keinanen et al. [32]. A ligand binds to the cleft of the LBD constructed between the two sub-domains called D1 and D2. The LBD is composed of two discontinuous polypeptides called S1 and S2, which are linked between LYS506 and PRO632 with the two artificial linker residues of GLY and THR. These artificial linker residues were added for the X-ray crystal structure analysis by Armstrong et al. [11]. A disulfide (S–S) bond is formed between CYS718 and CYS773. This LBD is connected to the ATD at THR394 and to the transmembrane segments M1, M2, and M3 at LYS506, PRO632, and GLY774, respectively [11].

There are four missing residues at the N-terminal and two at the C-terminal in the PDB structure (PDB: 1FTO), but we did not reconstruct any of these except for the GLY774 located at the C-terminal. The total number of residues was 258. The missing atoms and hydrogen atoms were rebuilt appropriately by using the LEaP module in the AMBER9 program [33]. The Parm96 in AMBER force field [34] and the TIP3P model for the explicit water molecules [35] were employed. We used two different systems in our MD simulations: one has an LBD in a water box without a glutamate (hereafter called SYS_1), and the other has an LBD in a water box with four glutamates (SYS_2). SYS_1 was used for the examination of the inter-domain motions in the apo state, and it was also used for the preparation of the initial structures to use in SYS_2. The unbiased binding MD simulations were performed using SYS_2 to investigate the process of the glutamate-binding into the LBD and that of the subsequent cleft closure.

The width of the cleft of LBD in the apo state fluctuates more than that in the glutamate-bound state [25]. In Lau's study, the free energy profile of the opening and closing of the cleft by the two-dimensional potential of mean force (PMF) was analyzed with the reaction coordinates of $\xi1$ and $\xi2$, which will be defined later, by the steered molecular dynamics (SMD) simulations [36,37] with the umbrella sampling method [38]. The accessible range was analyzed in terms of the one-dimensional reduced coordinate $\xi12 = (\xi1 + \xi2)/2$. Following these results, we selected the initial LBD structures for the binding simulations within the accessible range at body temperature. Because the width of the cleft is thermally fluctuating, the structures of the LBD with the cleft widely open are the preferable choice for the initial conditions.

For SYS_1, the protein structure obtained by the method described above was energy-minimized in a vacuum to avoid unfavorable atomic contacts. Then, only the LBD without any ion was solvated in a water box under the periodic boundary conditions. Adding ions to neutralize the system might enhance the artifacts, because the electrostatic field would be dramatically changed depending on the positions of the added ions. To avoid this, we used a method included in the sander module of AMBER9 [33] to neutralize the system by redistributing the excessive charges to the partial charges on all atoms in the system. This method has the merit of avoiding the collapse of the particle

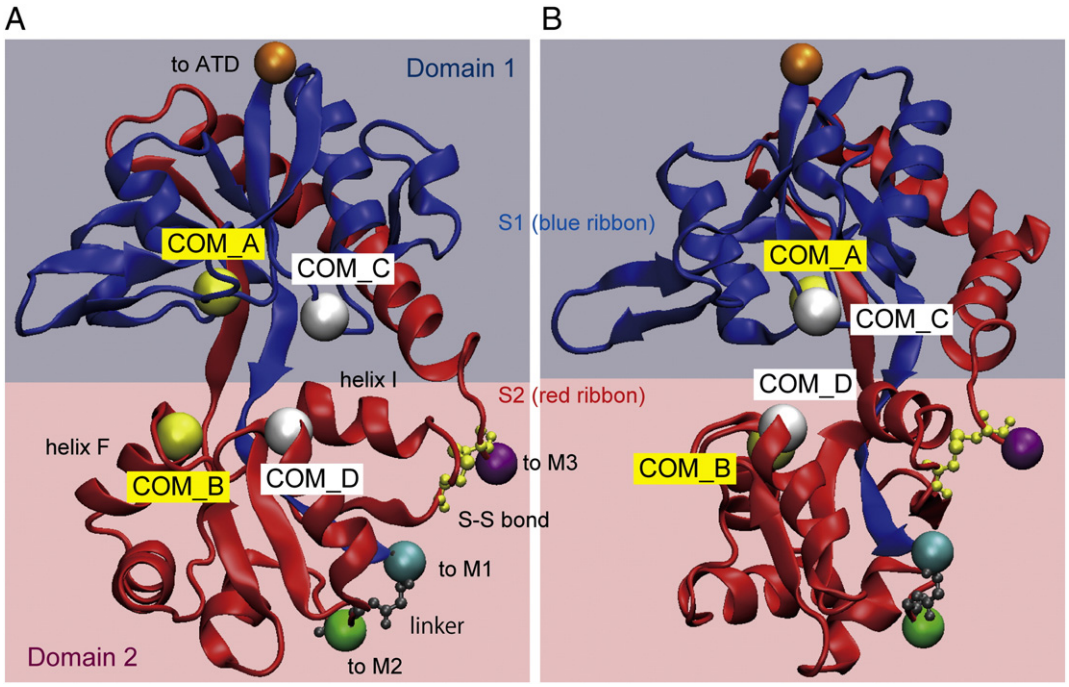

Fig. 1. Tertiary structure of the LBD of GluR2. (A) and (B) are viewed from different directions. Two discontinuous polypeptide segments designated S1 (a blue ribbon) and S2 (a red ribbon) form the D1 and D2 sub-domains set on light blue and pink rectangles, respectively. A ligand binds to the cleft constructed between D1 and D2. Linker residues (as shown by a gray ball and stick model) of GLY and THR were artificially introduced between LYS506 (its alpha carbon is depicted by a light blue ball) and PRO632 (a green ball), both of which were disconnected from the transmembrane segments M1 and M2, respectively. The ATD and the transmembrane segment M3 were disconnected from D1 at THR394 (an orange ball) and from D2 at GLY774 (a purple ball), respectively. A disulfide (S – S) bond is formed between CYS718 and CYS773 (shown by a small yellow ball and stick model). Four centers of mass of groups (large white and yellow balls), each of which is composed of two or three residues, are defined to analyze the inter-domain motions. COM_A: residues 479–481; COM_B: 654–655; COM_C: 401–403; and COM_D: 686–687.

mesh Ewald calculation [39] due to non-neutrality for the evaluation of the electrostatic interaction. The total numbers of atoms and water molecules in SYS_1 are 42,039 and 12,107, respectively.

To observe the binding process of the glutamate, 16 LBD structures with a one-dimensional reduced coordinate ξ12 of 15.5 Å were extracted from the trajectory with water molecules. We placed four glutamate molecules randomly around the jaws of the cleft of the prepared initial structures with a distance of more than 5 Å from the LBD to the glutamates artificially in SYS_2. For all 16 structures extracted from the trajectory, 16 different arrangements of the four glutamates were generated to obtain 256 different initial structures for the binding MD simulations. The water molecules within 5 Å from the glutamates were removed. The previous quantum mechanical calculations showed that the electrostatic interaction between the LBD and glutamate becomes significant at about 5 Å, suggesting that diffusing glutamates within about 5 Å from the protein are captured readily by residues via electrostatic interaction [40]. These results indicated that the distance of about 5 Å between the LBD and the glutamates is reasonable for the initial arrangements of the glutamates. The total charge in SYS_2 with one LBD and four glutamates was zero, and thus we did not have to redistribute the partial charges to neutralize the system. As we used many different initial structures, the total numbers of water molecules in SYS_2 were different from each other. The approximate total number of atoms was 40,200 in SYS_2.

2.2. MD simulations

The conditions of MD simulations for the systems SYS_1 and SYS_2 are explained below. The particle mesh Ewald method [39] was used to evaluate the electrostatic interactions. The SHAKE algorithm [41] was employed to apply constraints to all bonds with a hydrogen atom. The time step was 2 fs. The temperature was controlled by Berendsen's method [42], and the pressure was regulated at 1 atm by Andersen's method [43]. The temperature of SYS_1 was gradually raised from 100 K to 310 K in 180 ps. A 20-ns MD run was performed at 310 K to equilibrate the system and to investigate the inter-domain motions of the LBD in the apo state. The temperature of SYS_2 was raised from 100 K to 300 K in 120 ps, and then the temperature was raised to 310 K for the binding MD runs for 2 ns. When the glutamate successfully bound in the cleft of the LBD, such runs were extended to observe the closing process of the cleft. As the binding process is a stochastic and rare event for the time-consuming MD simulations, we tried many runs using different initial structures of the LBD as well as using different initial orientations and positions of glutamates with respect to the LBD.

The previous study calculated the PMF to analyze the free energy profile of the opening and closing of the cleft in the LBD [25]. Two-dimensional (2D) order parameters, ξ1 and ξ2, were defined as follows: ξ1 describes the distance between the centers of mass (COMs) of residues 479–481 (hereafter called COM_A) and 654–655 (COM_B), and ξ2 describes the distance between the COMs of residues 401–403 (COM_C) and 686–687 (COM_D) (Fig. 1A). The COMs were located almost in the same plane in the crystal structure in the apo state (PDB: 1FTO, chain-A) (Fig. 1B). In addition to the 2D order parameters, a one-dimensional reduced coordinate ξ12 was used (as defined earlier). Lau et al. estimated that 91% of the conformational ensemble was included within the range of $\Delta G(\xi 12) < 1.0$ kcal/mol, corresponding to the conformational space within the range of $11.1 < \xi 12 < 15.4$ Å at 300 K [25]. This range of the conformational space showed the accessible state of the LBD at 300 K. This is the reason why we extracted the structures with ξ12 of 15.5 Å from the trajectory of the 20-ns MD run at 310 K.

We used a Linux PC cluster composed of 4 nodes with 16 cores in total. Visualization tools called VMD (Visual Molecular Dynamics) [44] and DS Visualizer (Accelrys Software Inc., San Diego, CA, USA) were used to draw the molecular models.

2.3. Targeted MD simulations

We reproduced the closure of the LBD after the binding of the glutamate into the cleft. Using the structures extracted from the trajectory, in which the glutamate bound into the cleft and then the cleft closed spontaneously, we performed the targeted MD simulations with the sander module included in AMBER9 [33] to evaluate the free energy profile of the glutamate-binding and cleft-closing processes. The root mean square deviation (RMSD) from the glutamate-bound X-ray crystal structure of GluR2 (PDB: 1FTJ, chain-A) was defined as the reaction coordinate. The initial structures on the reaction coordinate were manually selected to have an RMSD interval of 0.1 Å from 1.1 to 4.8 Å. Harmonic potentials were introduced to control the RMSD of the alpha carbon atoms of the LBD and the atoms except for the hydrogen in the glutamate. The RMSD fluctuated around the initial value in each time window appropriately with a force constant of 0.01 kcal/(mol × Å^2 × atom number) for all windows except four windows with the RMSD between 1.1 and 1.4 Å, where we used 0.1 kcal/(mol × Å^2 × atom number). Each window was simulated for 1.2 ns including the first 0.2 ns equilibration run following the calculation conditions employed by Noy et al [45]. We obtained a smooth transition and good overlap between windows by using these conditions. The PMF was calculated using the WHAM method [46] and the program provided by Alan Grossfield [47].

3. Results

3.1. Inter-domain motion of the ligand-binding domain in the apo state

3.1.1. Root mean square deviations of the ligand-binding domain from the apo crystal structure

Inter-domain motion in the apo state was examined using the RMSDs from the apo crystal structure (PDB: 1FTO, chain-A). The time evolution of the RMSD of the whole protein (Fig. 2A) was calculated using the coordinates of the alpha carbon atoms in the whole protein at 310 K for 20 ns. The time evolutions of the RMSDs of D1 (Fig. 2B) and D2 (Fig. 2C) were calculated using the trajectories of the alpha carbon atoms of D1 and D2, respectively, at 310 K for 20 ns. The RMSD of the whole protein fluctuates between 1.0 and 2.0 Å during the first 7 ns and between 1.5 and 3.0 Å for most of the remaining 13 ns with some sporadic increases to more than 3.0 Å. We used the part of the trajectory between 7 and 20 ns for the analyses of inter-domain motion in the apo state, because the fluctuation of the LBD in the apo state reported by Arinaminpathy et al. [19] was in the same range of 1.5–3.0 Å. The RMSDs of the D1 and D2 fluctuate between 1.0 and 1.5 Å for the first 7 ns and between 1.5 and 2.0 Å for the remaining 13 ns.

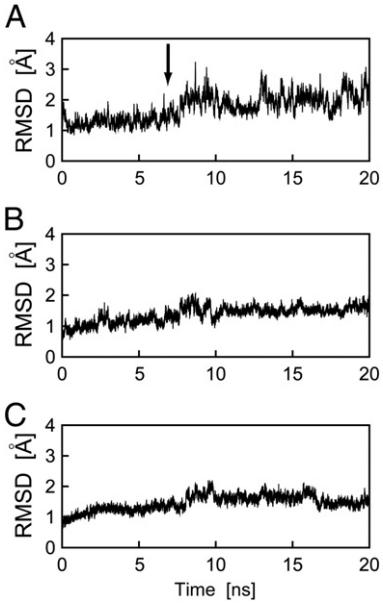

Fig. 2. Time evolutions of RMSD from the crystal structure in the apo state (PDB: 1FTO, chain-A) calculated using the alpha carbon atoms. (A) Time evolution for the whole protein for 20 ns. (B) That for D1; and (C) that for D2. The arrow in (A) shows a large change in the RMSD.

3.1.2. Changes in distances and angles of the centers of mass of residues for examination of molecular motions

The inter-domain motion was examined directly by the changes in distances and angles defined by the COMs that were composed of two or three residues (Fig. 3A). The fluctuations of the distances during the first 7 ns were also smaller than those during the remaining 13 ns, showing that the trends of the fluctuations in terms of time are similar to those of the RMSDs as mentioned above. The probability density was investigated by the distribution of ξ1 and ξ2 (Fig. 3B). We found that the shape of the distribution was oval and that there was a positive correlation between ξ1 and ξ2 with a correlation coefficient of 0.56. Such an oval shape indicates that the biased fluctuation took place between two sub-domains.

We evaluated the distances of the other pairs of COMs of residues in the different sub-domains. We defined the distances between COM_A and COM_D and between COM_B and COM_C as ξ3 and ξ4, respectively. We calculated the time evolutions and the distributions of ξ3 and ξ4 (Fig. 3C,D). There seemed to be no correlation between ξ3 and ξ4 based on the correlation coefficient of −0.13.

To investigate the twist motion, we evaluated the distributions of the angles composed of the COMs as explained below. We calculated the distribution of the pair of angles, COM_A-COM_B-COM_D (angle_1) and COM_C-COM_A-COM_B (angle_3) (Fig. 3E). There was a negative correlation with a correlation coefficient of −0.65. The distribution of the pair of angles, COM_B-COM_D-COM_C (angle_2) and angle_3, showed a positive correlation with a correlation coefficient of 0.74 (Fig. 3F). These results showed that twist motion took place between the two sub-domains D1 and D2.

3.1.3. Large-scale motion of the ligand-binding domain in the apo state by principal component analysis

The large-scale motion of the backbone of the protein can be analyzed by principal component analysis (PCA) [48–50] using the trajectories obtained by the MD simulations. In PCA, after the translational and rotational motions are removed from the trajectory, a variance-covariance matrix is calculated using the coordinates of the alpha carbon atoms and then diagonalized to obtain the eigenvalues and eigenvectors. The first principal mode with the smallest eigenvalue represents the largest motion, which is generally thought to be of great importance for the function of the protein. In the first principal mode in our MD simulations, the hinge-like motion was clearly observed, suggesting that the opening and closing motion of the cleft of GluR2 took place (Fig. 4A). The second principal mode clearly indicated a twist motion between D1 and D2 (Fig. 4B).

3.1.4. Conformational change clarified by comparison of the X-ray crystal structures of the apo and glutamate-bound states

The structural change was investigated by HINGEFIND [51] using two X-ray crystal structures in the apo (PDB: 1FTO, chain-A) and the glutamate-bound (PDB: 1FTJ, chain-A) states. These structures were superposed with respect to the alpha carbon atoms in D1 (Fig. 4C,D; these two panels present views from different directions). The hinge-like structural change in the first principal mode was obtained in the superposed structures by HINGEFIND (Fig. 4D), and the twist structural change was also recognized in the superposed structures (Fig. 4C). These hinge-like and twist structural changes

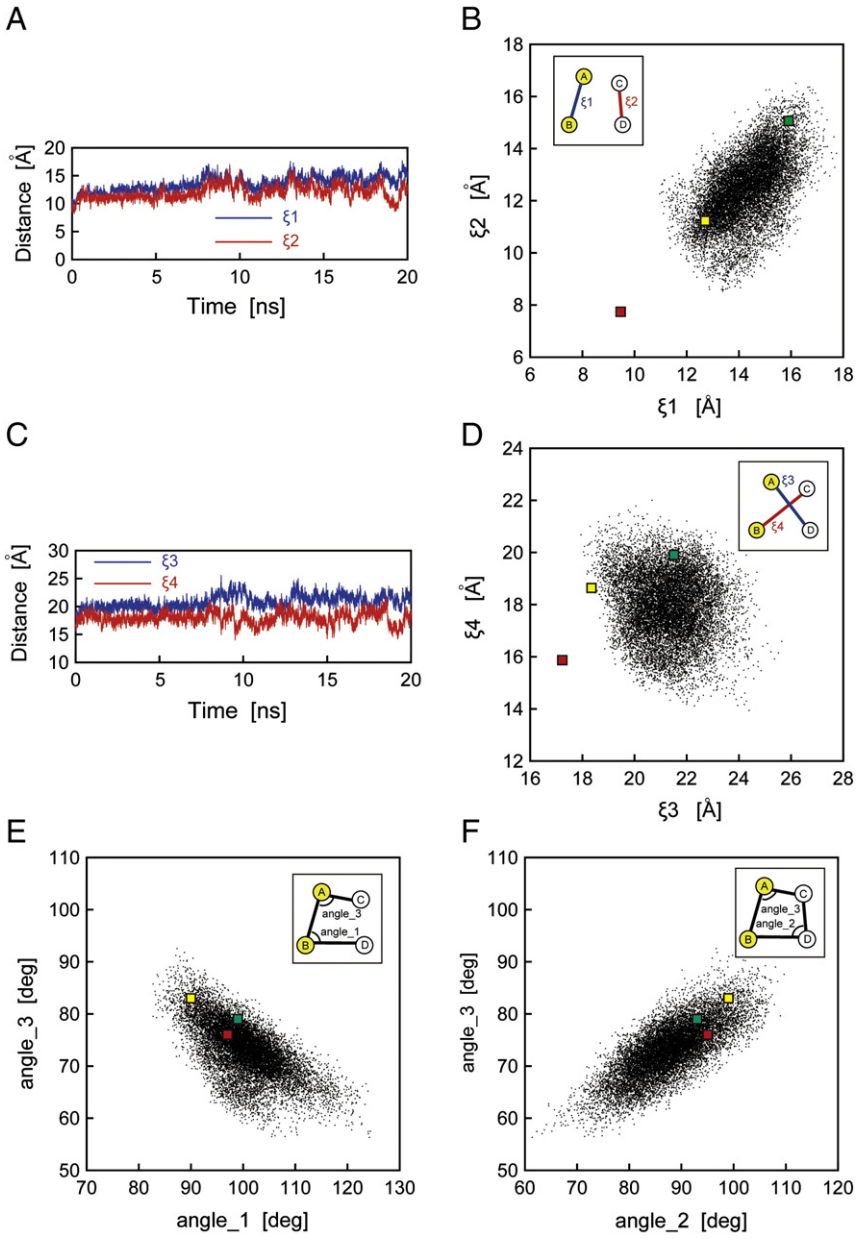

Fig. 3. Time evolutions and distributions of the distances and angles defined by the COMs in the apo equilibrium state. The distributions are plotted using the trajectory of the atoms between 7 and 20 ns for every 1 ps. (A) Time evolutions of ξ1 (blue) and ξ2 (red). (B) Distribution of ξ1 and ξ2. (C) Time evolutions of ξ3 (blue) and ξ4 (red). (D) Distribution of ξ3 and ξ4. (E) Distribution of angle_1 and angle_3. (F) Distribution of angle_2 and angle_3. The green rectangles in the distributions (B, D, E, F) represent the initial pairs of distances and angles used in the binding simulation, where the glutamate-bound and the cleft-closure structures were observed. In (B), (D), (E), and (F), the pairs of the distances and angles in the apo crystal structure (PDB: 1FTO, chain-A) and in the glutamate-bound structure (PDB: 1FTJ, chain-A) are plotted by yellow and red rectangles, respectively. The insets in (B), (D), (E), and (F) are the schematics of the distances and angles defined by COMs.

are thought to be related to the opening and closing of the ion channel pore formed by the four iGluRs [11].

The results of RMSDs, the distributions of the distances, and the first and second principal modes obtained by our MD calculations in the equilibrium apo state agree well with the reported results [19,25,28]. These results convinced us to use our MD system for the binding MD simulations as explained below.

3.2. Glutamate-binding and cleft-closing processes

3.2.1. Binding of glutamate to the ligand-binding domain

We performed the MD calculations without employing any artificial constraints in order to observe the glutamate-binding and cleft-closing processes. In 6 out of 256 MD runs for 2 ns at 310 K, 1 of the 4 glutamates in SYS_2 bound to the cleft of the LBD spontaneously. We observed the spontaneous closure of the cleft in only 1 out of the 6 runs in 20 ns. The LBDs in the other 5 runs did not reach the closed state in 20 ns, because the time required to close the cleft depends on the initial arrangements and motions of the molecules in the system used in the MD simulations. To avoid the possibility that the closure of the cleft occurred by chance in the relatively short period of time in our simulation, we continued to analyze the precise glutamate-binding and cleft-closing processes by extending our calculations using the cleft-closed run up to 40 ns. The initial distances of ξ1, ξ2, ξ3, and ξ4 were 15.9, 15.1, 21.5, and 19.9 Å, respectively. The initial values of angle_1, _2, and _3 were 94.6, 92.9, and 78.6 degrees, respectively. All of the initial distances and angles ranged within the distributions in the apo equilibrium state (Fig. 3B,D,E,F).

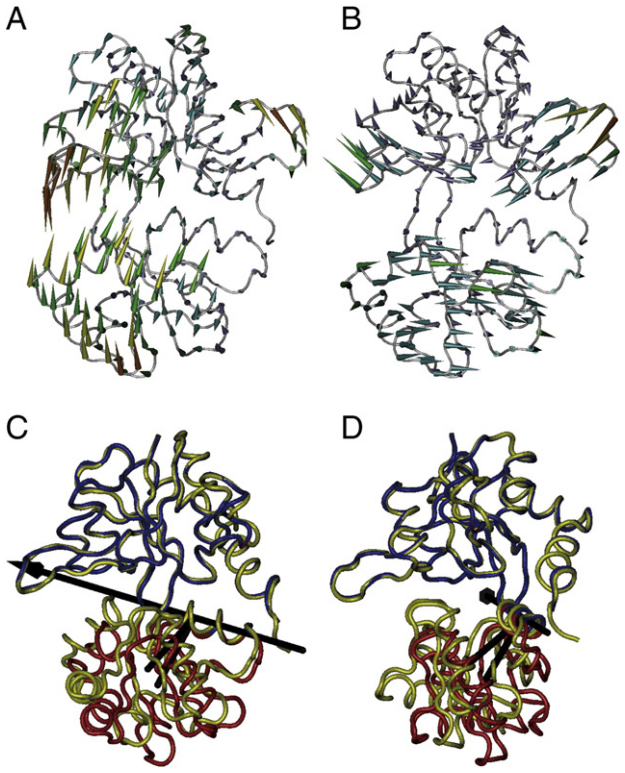

Fig. 4. Conformational changes of the LBD of GluR2. (A and B). The first (A) and second (B) principal modes corresponding to the two largest motions obtained by PCA are depicted by cones on the alpha carbon atoms. The color and length of the cones represent the magnitude of the motion. Warm colors indicate the magnitude of a large motion, and cold colors indicate the magnitude of a small motion. (C and D) The apo open (PDB: 1FTO, chain-A, D1: blue; D2: red) and glutamate-bound closed (PDB: 1FTJ, chain-A, yellow) structures were superposed with respect to the alpha carbon atoms in D1 that were analyzed by HINGEFIND. (C) and (D) present views from different directions to enable us to see the structural changes clearly. The long black arrow represents the rotation axis. The centers of mass of D2s in the apo and glutamate-bound states are connected perpendicularly to the rotation axis by the two small black sticks. The angle between the two sticks is 19°.

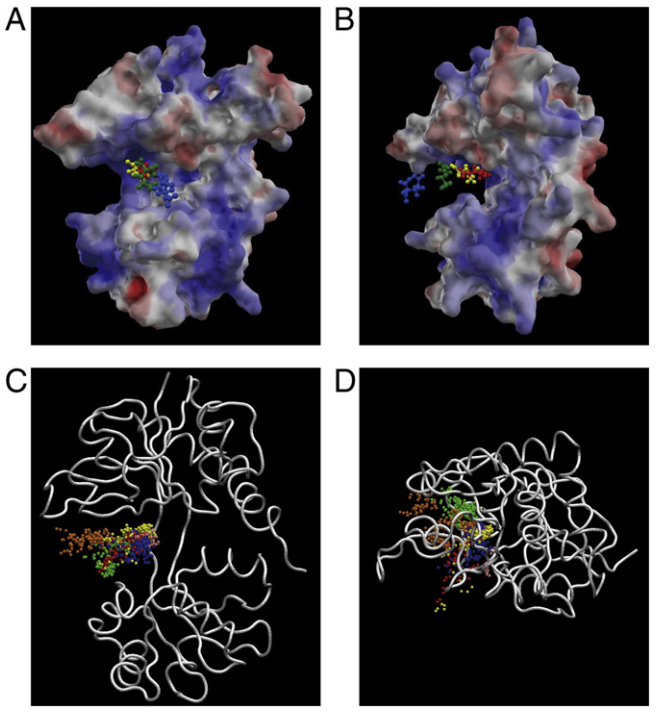

Fig. 5. Glutamate-binding paths in the cleft. (A and B) Electrostatic field on the surface of LBD calculated by eF-surf. These two panels present views from different directions. The color varies from red (−0.1 V) to blue (+0.1 V). The positions of the glutamate bound to the cleft followed by the cleft-closure are shown by different colors with respect to time at 0 ps (blue), 70 ps (green), 150 ps (yellow), and 300 ps (red). (C and D) Six different sets of binding paths in which one glutamate was calculated in an MD run. The difference among these six sets refers to the different initial positions shown by the different colors. The balls express the positions of the beta carbon atoms of the glutamates, because the beta carbon atom locates near the center of the glutamate.

3.2.2. Binding path of glutamate into the ligand-binding domain

The binding path of the glutamate was analyzed using the trajectories obtained from the MD simulations (see Supplementary movies). In the cleft-closed trajectory, the glutamate initially underwent a slight change in orientation at the jaws of the cleft and within 300 ps it advanced deeply into the cleft (Fig. 5A,B). In the other five MD trajectories starting from the different initial structures, the glutamate bound to the cleft successfully but the cleft did not close within 20 ns. In all these trajectories, the glutamate bound to the cleft through the left side of the LBD (see Fig. 5C,D) within 1 ns from the outside of the cleft. The initial distances between the LBD and the glutamates were more than 5 Å.

The electrostatic field at the surface of the atoms of LBD was obtained with eF-surf [52] (Fig. 5A,B; the two panels present views from different directions). The glutamate seemed to enter into the cleft due to the strong attractive force of the positive electrostatic field originating from the atoms of the cleft of LBD.

3.2.3. Closure of the cleft by glutamate binding

The time evolution of RMSD of the alpha carbon atoms in the LBD from the glutamate-bound crystal structure (PDB: 1FTJ, chain-A) was examined for clarification of the closure mechanism of the cleft (Fig. 6A). The RMSD decreased from 5.0 to 2.3 Å in 1 ns, and then it fluctuated up to 15 ns in another state that was expected to exist between the open and closed states. This state is referred to as a "semi-open" state. Finally, at 15 ns, the RMSD reached 1.5 Å, indicating that the structure of LBD at this time point was similar to that of the glutamate-bound X-ray crystal structure in the closed state (Fig. 6A). Similar to the time evolutions of the RMSD, both the distances ξ1 and ξ2 decreased rapidly in 1 ns after the entry of the glutamate into the cleft at 300 ps. Both distances maintained constant values of 12 Å up to 15 ns in this semi-open state, before they decreased to 9.6 Å (ξ1) and 9.0 Å (ξ2) to induce the closed state. These distances agree with the reported distances of 9.4 Å (ξ1) and 8.4 Å (ξ2) at the most stable state of the glutamate-bound structure in the free energy profile calculated by the previous MD simulation at 300 K [25] and with those of 9.5 Å (ξ1) and 7.8 (ξ2) Å in the glutamate-bound X-ray crystal structure (PDB: 1FTJ, chain-A) that was measured at 110 K.

Because three pairs of residues, (GLU402, THR686), (GLY451, SER652), and (GLU705, TYR732), have been expected to play important roles in the closure of the cleft based on the previous MD simulation [53], the structure at 35 ns of our binding MD simulation and the glutamate-bound crystal structure (PDB: 1FTJ, chain-A) were superposed by minimizing the RMSD of the alpha carbon atoms in the cleft between these two structures (Fig. 7A). The whole structure obtained by our MD simulation was similar to the glutamate-bound X-ray crystal structure, but only the (GLY451 and SER652) pair of residues failed to form a complete hydrogen bond with the average distance of 6.0 Å. In particular, the glutamate-bound structure of the cleft in our MD simulation was in excellent agreement with the X-ray co-crystal structure (PDB: 1FTJ, chain-A) (Fig. 7B). Most of the hydrogen bonds observed in the X-ray co-crystal structure were reproduced in the structure obtained by our MD simulations.

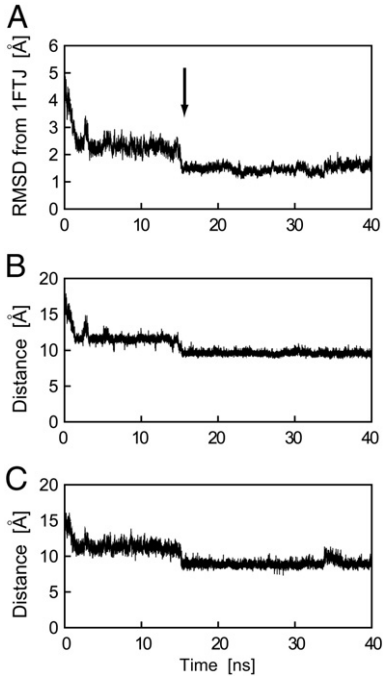

Fig. 6. Time evolutions of RMSD and distances of the two sub-domains. (A) Time evolution of the RMSD of the alpha carbon atoms from the glutamate-bound crystal structure (PDB: 1FTJ, chain-A) in the glutamate-bound and cleft-closed MD simulation. (B and C) Time evolutions of the distances ξ1 (B) and ξ2 (C) in the glutamate-bound and cleft-closed MD simulation. The arrow shows that there was a transition from the semi-open state to the closed state.

3.2.4. Hydrogen bonds in the glutamate-bound structure

We analyzed the roles of the residues of GluR2 in the detailed processes of the glutamate binding and the cleft closure. The time evolutions of the distances were examined over a period of 40 ns between the atoms of the glutamate and those of ARG485, THR480, and PRO478 in D1, and GLU705, SER654, and THR655 in D2 (Supplementary Fig. 1A). The atoms of these amino acids are known to form the hydrogen bonds in the glutamate-bound X-ray crystal structure (PDB: 1FTJ). The glutamate formed the hydrogen bonds with ARG485, THR480, PRO478, and GLU705 within 1 ns. However, it took about 15 ns to form both the hydrogen bond between the glutamate and SER654 and that between the glutamate and THR655. When we noted the time evolutions of the distances between the glutamate and the residues ARG485, THR480, PRO478, TYR450, and GLU705 for 1.5 ns (Supplementary Fig. 1B), the alpha carboxyl group of the glutamate was attracted to the distance 5.0 Å at 150 ps from the guanidine of ARG485 by the electrostatic interaction. Then, the glutamate formed the hydrogen bonds with ARG485, THR480, and PRO478 at 300 ps simultaneously.

At 1 ns, the amino group of glutamate was attracted to the carboxyl group of GLU705 by the electrostatic interaction, and they formed a hydrogen bond. ARG485, THR480, PRO478, and GLU705 are in the glutamate-binding site, and they are conserved in many iGluRs [25]. These facts suggest that one of the roles of these residues is to attract the glutamate into the cleft. At this time point, the distances of ξ1 and ξ2 were both about 12 Å (Fig. 6B,C), and the RMSD from the glutamate-bound X-ray crystal structure (PDB: 1FTJ, chain-A) was more than 2 Å (Fig. 6A). These results strongly support that there is a "semi-open" state between the open and closed states. The time evolutions of the distances were examined between the pairs of residues that are thought to be important for the cleft closure (Supplementary Fig. 2). The hydrogen bond between TYR732 and GLU705 was formed at 1 ns, and that between THR686 and GLU402 was formed at 15 ns. However, no hydrogen bond was formed between GLY451 and SER652 within 40 ns.

3.2.5. Distance change between TYR450 and glutamate in the glutamate-binding process

The distance change was examined between the nitrogen atom of the glutamate and the gamma carbon atom of TYR450 (Supplementary Fig. 1B). The protonated amino group of the glutamate with a positive charge was positioned near the benzene ring of TYR450 with a distance of 3.0 Å at 250 ps. However, the distance increased to 5 Å after 300 ps due to the deeper binding of the glutamate into the binding site. The orientation of the glutamate seemed to be controlled by the space molded by the benzene ring of TYR450 and also controlled by a so-called cation–π attractive interaction between the amino group of the glutamate and the benzene ring of TYR450.

3.2.6. Hydrogen bonds between LYS730 and GLU705 and between LYS730 and ASP728

LYS730 has been proposed to switch its hydrogen-bond partner from GLU705 to ASP728 based on a comparison of the crystal structures in the apo and glutamate-bound states [11]. The time evolutions of the distances were examined between the amine nitrogen in LYS730 and the carboxyl oxygen in GLU705 and also between the amine nitrogen in LYS730 and the carboxyl oxygen in ASP728 for the deformation and formation of the hydrogen bonds (Supplementary Fig. 2). LYS730 formed a hydrogen bond with GLU705 in the initial structure. Then, LYS730 cut this hydrogen bond but formed a new hydrogen bond with ASP728 at about 250 ps upon glutamate binding. The hydrogen bond between LYS730 and ASP728 was maintained until at least 40 ns. The distance between the amine nitrogen in LYS730 and the carboxyl oxygen in GLU705 became constant after GLU705 formed the hydrogen bond with the glutamate at 1 ns (Supplementary Fig. 1B).

3.2.7. Potential of the mean force in the glutamate-binding and cleft-closing processes

We evaluated the PMF along the reaction coordinates defined by the RMSD of the LBD from the glutamate-bound X-ray crystal structure (PDB: 1FTJ, chain-A) (Fig. 8). We used the 38 structures from 1.1 to 4.8 Å in the RMSD with an interval of 0.1 Å obtained by the MD run, in which the glutamate bound to the cleft, resulting in the closure of the cleft. The RMSD value at the minimum PMF obtained by the MD simulations at 310 K was not 0.0 Å but 1.5 Å probably due to the thermal fluctuation and the differences in temperature, when the X-ray experiment was done at 110 K (PDB: 1FTJ). That is, the RMSD with the lowest PMF was shifted from 0.0 to 1.5 Å by the thermal fluctuation to have a low probability density in the range smaller than 1.5 Å. The sharp rise occurring at 4.8 Å was an artifact that came from the upper termination range of 4.8 Å for the umbrella sampling, where the region beyond the upper limit was not sampled (Fig. 8). The two large peaks were obtained at 1.7 and 3.1 Å with the free energy barriers of 1 and 0.6 kcal/mol, respectively towards the direction to close the cleft. The peak at 1.7 Å corresponded to the decrease of the RMSD from 2.0 to 1.5 Å at 15 ns as shown in Fig. 6A. The other large peak at 3.1 Å corresponded to the initial decrease of the RMSD.

4. Discussion

We succeeded in observing the spontaneous glutamate-binding and cleft-closing processes in our MD simulations. We identified the "semi-open" state between the open state and the closed state in the calculated free energy profile. TYR450 seems to guide the glutamate to bind to the cleft appropriately by the cation–π attractive interaction formed by its benzene ring. The inter-domain hydrogen bond between GLU705 and TYR732 reinforces the structure in the semi-open state for the transition occurring before the closed state. The two hydrogen bonds of the glutamate with SER654 and THR655 as well as the inter-domain hydrogen bond between GLU402 and

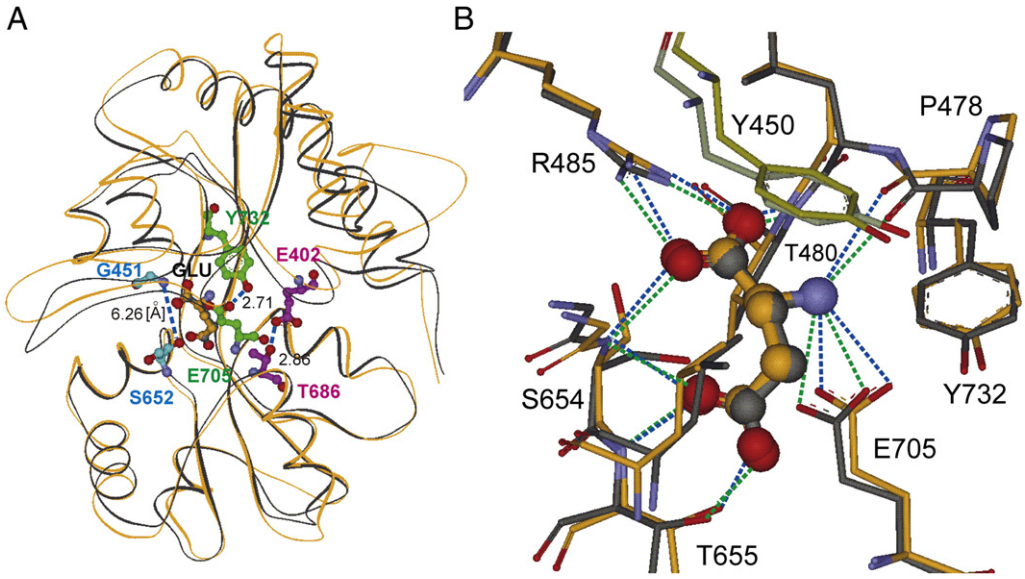

Fig. 7. Glutamate-bound structures superposed to the co-crystal structure in the closed state (PDB: 1FTJ, chain-A) calculated with respect to the alpha carbon atoms in the cleft. (A) The backbone structures of the LBDs depicted with orange (MD) and black (PDB: 1FTJ, chain-A) lines. The glutamate and three pairs of residues obtained by the MD calculation at 35 ns are represented with ball and stick models. Their carbon atoms are colored orange (glutamate), blue (GLY451 and SER652), green (TYR732 and GLU705), and pink (GLU402 and THR686). (B) The structures around the glutamate in the cleft with the hydrogen bonds. The blue and green dashed lines indicate the hydrogen bonds observed in the MD and the co-crystal structure, respectively. The carbon atoms obtained by the MD simulation at 35 ns are colored orange and those of the co-crystal structure (PDB: 1FTJ, chain-A) are colored gray.

THR686 are crucial for the transition from the semi-open state to the closed state.

4.1. Inter-domain motions of the ligand-binding domain in the apo state

The ranges of fluctuations of the RMSDs of D1 and D2 (Fig. 2B,C) were small, and they did not shift between 7 and 20 ns, indicating that the tertiary structures of both D1 and D2 were stable and relatively rigid. This suggests that the larger fluctuation of the RMSD of the whole protein is attributable to the inter-domain motion, which is crucial for the opening and closing of the iGluR ion channel. The stability during the first 7 ns of the MD simulation appeared to reflect the stability of the crystal structure.

The directions of the changes in the distributions of the distances and angles between the apo state (PDB: 1FTO, chain-A) and the glutamate-bound state (PDB: 1FTJ, chain-A) are similar to the directions in the biased fluctuation (Fig. 3B,E,F). This phenomenon supports *the general relationship between fluctuations and a response to a stimulus* [54,55], where the stimulus is the binding of the glutamate to the LBD in the present study.

The inter-domain motions obtained by the PCA (Fig. 4A,B) were also in accordance with the reported first-principal mode evaluated using many crystal structures of LBD of the GluR2 with a variety of ligands by Bjerrum et al. [26], as well as with the results of the PCA of the LBD of the NMDA receptor by Kaye et al. [28]. The structural changes by the inter-domain motion also agreed with those analyzed using the static X-ray crystal structures by HINGEFIND [51] (Fig. 4C,D).

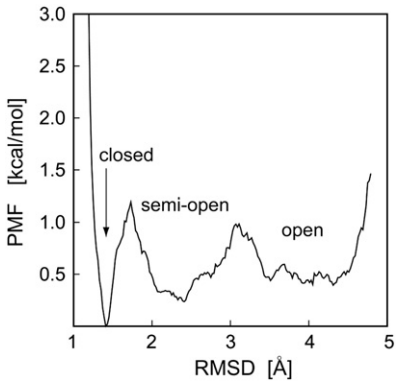

Fig. 8. Potential of mean force in terms of the RMSD of the alpha carbon atoms from the glutamate-bound crystal structure (PDB: 1FTJ, chain-A). The open, semi-open, and closed states are identified by the two transition states between them.

4.2. Glutamate-binding process

As this tyrosine is conserved in the LBD of many iGluRs [24], we speculate that one of the roles of the tyrosine at the center of the binding site is to guide the glutamate to enter the cleft appropriately.

The position of TYR450 is fixed by the hydrogen bond with GLU402, and its bulky benzene ring seems to mold the space for the glutamate to bind in the appropriate direction with the support of the cation–π attractive interaction. Although the accurate cation–π interaction has to be evaluated by quantum mechanical calculations, the standard force fields, especially their electrostatic components, can correctly reproduce trends of binding energies [56,57]. For this reason, we believe that the effect by the cation–π interaction is partially included in the MD calculations.

We believe that the electrostatic field originating from the LBD is the primary driving force for the binding of the glutamate to the cleft via the path on the left side of the LBD (Fig. 5A). Taking into account the fact that one side of the jaws is tightened by the disulfide bond at the edge of the cleft and the rigid transdomain β strand functions as a hinge by connecting the two sub-domains at the center of the LBD, the other side would be facilitated to open widely. These structural characteristics are also inferred from the superposed X-ray crystal structures in the open and closed states (Fig. 4C). Mamonova et al. showed that the helix I, which is in D2 and contains CYS718 at the edge, forming the disulfide bond with CYS773 in D1, is less mobile than other helices in D2 [52]. Their results suggest that the structure of the right side of the LBD

(Fig. 1A) is stiffer and harder to open than the other side, supporting the binding path clarified by our MD simulations.

4.3. Cleft-closing process

The formation of a hydrogen bond between TYR732 in D1 and GLU705 in D2 initiates the conformational change from the open state to the semi-open state, and the formation of a hydrogen bond between GLU402 and THR686 is related to the conformational change from the semi-open state to the closed state. The glutamate-bound crystal structure (PDB: 1FTJ) has three independent chains of the LBD in a unit cell, and the structures are slightly different from each other. The pairs of the residues (GLU705 and TYR732) and (GLU402 and THR686) form hydrogen bonds in all three chains. However, the distances between the nitrogen atom in GLY451 and the oxygen atom of the carbonyl group in SER652 are 5.35, 3.82, and 3.19 Å in the chain-A, -B, and -C, respectively, although they all exist in the closed states. That is, the hydrogen bonds are not formed in chain-A and -B completely. This suggests that the hydrogen bond between GLY451 and SER652 is not crucial for the LBD to form the closed state, and thus we have not obtained the hydrogen bond between these residues in the 40-ns MD run. Mamonova et al. pointed out that this hydrogen bond may play a role in rigidifying the structure of the complex for the tighter cleft closure [53].

We infer that one of the roles of GLU705 and TYR732, which are conserved in the LBD of many iGluRs, is to reinforce the semi-open state for the transition occurring before the closed state. We speculate that one of the roles of the residues SER654, THR655, THR686, and GLU402 is to transform the LBD from the semi-open state to the closed state.

Abele et al. have shown that the glutamate binds to D1 of the LBD rapidly followed by slower conformational change of the LBD by stop-flow experiment [58]. Cheng et al. have investigated the glutamate-binding and cleft-closing processes of GluR2 using time-resolved vibrational spectroscopy [59]. They showed that there is a partial cleft closure state after the binding of the alpha carboxyl group of the glutamate with ARG485 of D1, followed by the establishment of the interactions between the gamma carboxyl group of the glutamate and the residues in D2 to make a large conformational change. In our MD simulation glutamate bound to the cleft within 1 ns in six MD runs and the cleft closed within 20 ns in only one run among the six runs. We do not have to compare this cleft-closure time with the data observed by the experiments, because the present experimental techniques do not have an enough resolution of time, such as nanoseconds. That is, it is a future issue that opening and closing of 'one subunit cleft' can be detected by experiments. The multiple conformational states were reported to include glutamate-binding, domain-isomerization, and lobe-locking steps by hydrogen-deuterium exchange experiments [60]. The identification of the semi-open state in the present study agreed with these experimental results.

4.4. Potential of mean force in the glutamate-binding and cleft-closing processes

We assigned the structure between the two transition states at 1.7 Å and 3.1 Å as the semi-open state (Fig. 8). The transition from the open state to the semi-open state was faster than that from the semi-open state to the closed state, probably because the barrier at 3.1 Å in the RMSD in the PMF was lower than that at 1.7 Å. Although Noy et al. pointed out that the current target MD simulations cannot be used to determine precisely the free energy barrier at the large conformation of DNA [44], the barriers of 1 and 0.6 kcal/mol were clearly observed in the present study. The existence of the semi-open state can also be speculated from the constant values of the RMSD at 2.2 Å from 2 to 15 ns (Fig. 6A). The semi-open state was also identified by targeted and multi canonical MD calculations, although the existence of the glutamate was not considered [61]. For this reason the minimum energy of the PMF in their results is not in the closed state but in the open state. However, the overall PMF profile obtained in their studies agrees well with our results. This supports the existence of the semi-open state in glutamate-binding and cleft-closing processes. Because we obtained the results with only one trajectory, further investigations are needed to discuss this issue precisely.

5. Conclusion

The accordance observed between the direction of the biased fluctuation in the apo equilibrium state and that of the cleft-closure state supports the notion of a general relationship between the fluctuation and a response to a stimulus. We speculated that one of the roles of TYR450 is to guide the regulation of the orientation of the glutamate upon binding by its benzene ring to induce the cation–π attractive interaction. To our knowledge, this is the first successful calculation of the potential of mean force based on the structures on the spontaneously ligand-bound and cleft-closed pathway by the unbiased MD simulations. We identified the semi-open state between the open state and the closed state. GLU705 in D2 forms a hydrogen-bond bridge with TYR732 in D1, presumably reinforcing the semi-open structure for the transition occurring before the closed state.

Supplementary data associated with this article can be found, in the online version, at doi:10.1016/j.bpc.2011.12.004.

Acknowledgments

We thank Dr. Hideo Kubodera for his helpful discussion and manuscript revision. We also thank Dr. Kazuo Suzuki for his continuing encouragement.

References

[1] R.E. Oswald, Ionotropic glutamate receptor recognition and activation, Advances in Protein Chemistry 68 (2004) 313–349.
[2] S.E. Traynelis, L.P. Wollmuth, C.J. McBain, F.S. Menniti, K.M. Vance, K.K. Ogden, K.B. Hansen, H. Yuan, S.J. Myers, R. Dingledine, Glutamate receptor ion channels: structure, regulation, and function, Pharmacological Reviews 62 (2010) 405–496.
[3] R. Dingledine, K. Borges, D. Bowie, S.F. Traynelis, The glutamate receptor ion channels, Pharmacological Reviews 51 (1999) 7–61.
[4] K.L. Mayer, N. Armstrong, Structure and function of glutamate receptor ion channels, Annual Review of Physiology 66 (2004) 161–181.
[5] M.L. Mayer, Glutamate receptors at atomic resolution, Nature 440 (2006) 456–462.
[6] A.I. Sovolevsky, M.P. Rosconi, E. Gouaux, X-ray structure, symmetry and mechanism of an AMPA-subtype glutamate receptor, Nature 462 (2009) 745–756.
[7] P.H. Seeburg, The TINS/TiPS lecture the molecular biology of mammalian glutamate receptor channels, Trends in Neurosciences 16 (1993) 359–365.
[8] M. Hollmann, S. Heinemann, Cloned glutamate receptors, Annual Review of Neuroscience 17 (1994) 31–108.
[9] S. Ozawa, H. Kamiya, K. Tsuzuki, Glutamate receptors in the mammalian central nervous system, Progress in Neurobiology 54 (1998) 581–618.
[10] N. Armstrong, Y. Sun, G.Q. Chen, E. Gouaux, Structure of a glutamate-receptor ligand-binding core in complex with kainite, Nature 395 (1998) 913–917.
[11] N. Armstrong, E. Gouaux, Mechanisms for activation and antagonism of an AMPA-sensitive glutamate receptor: crystal structures of the GluR2 ligand binding core, Neuron 28 (2000) 165–181.
[12] A. Hogner, J.S. Kastrup, R. Jin, T. Liljefors, M.L. Mayer, J. Egebjerg, I.K. Larsen, E. Gouaux, Structural basis for AMPA receptor activation and ligand selectivity: crystal structures of five agonist complexes with the GluR2 ligand-binding core, Journal of Molecular Biology 322 (2002) 93–109.
[13] R. Jin, M. Horning, M.L. Mayer, E. Gouaux, Mechanism of activation and selectivity in a ligand-gated ion channel: structural and functional studies of GluR2 and quisqualate, Biochemistry 41 (2002) 15635–15643.
[14] C. Kasper, K.L. Lunn, T. Liljefors, E. Gouaux, J. Egebjerg, J.S. Kastrup, GluR2 ligand-binding core complexes: importance of the isoxazolol moiety and 5-substituent for the binding mode of AMPA-type agonists, FEBS Letters 531 (2002) 173–178.
[15] A. Hogner, J.R. Greenwood, T. Liljefors, M.L. Lunn, J. Egebjerg, I.K. Larsen, E. Gouaux, J.S. Kastrup, Competitive antagonism of AMPA receptors by ligands of different classes: crystal structure of ATPO bound to the GluR2 ligand-binding core, in comparison with DNQX, Journal of Medicinal Chemistry 46 (2003) 214–221.
[16] R. Jin, T.G. Banke, M.L. Mayer, S.F. Traynelis, E. Gouaux, Structural basis for partial agonist action at ionotropic glutamate receptors, Nature Neuroscience 6 (2003) 803–810.
[17] K. Menuz, R.M. Stroud, R.A. Nicoll, F.A. Hays, TARP auxiliary subunits switch AMPA receptor antagonists into partial agonists, Science 318 (2007) 815–817.

[18] J. Mendieta, G. Ramírez, F. Gago, Molecular dynamics simulations of the conformational changes of the glutamate receptor ligand-binding core in the presence of glutamate and kainite, Proteins 44 (2001) 460–469.
[19] Y. Arinaminpathy, M.S.P. Sansom, P.C. Biggin, Molecular dynamics simulations of the ligand-binding domain of the ionotropic glutamate receptor GluR2, Biophysical Journal 82 (2002) 676–683.
[20] M. Kubo, E. Shiomitsu, K. Odai, T. Sugimoto, H. Suzuki, E. Ito, Picosecond dynamics of the glutamate receptor in response to agonist-induced vibrational excitation, Proteins 54 (2004) 231–236.
[21] M. Kubo, E. Ito, Structural dynamics of an ionotropic glutamate receptor, Proteins 56 (2004) 411–419.
[22] J. Mendieta, R. Gago, G. Ramírez, Binding of 5′-GMP to the GluR2 AMPA receptor: insight from targeted molecular dynamics simulations, Biochemistry 44 (2005) 14470–14476.
[23] Y. Arinaminpathy, M.S. Sansom, P.C. Biggin, Binding site flexibility: molecular simulation of partial and full agonists within a glutamate receptor, Molecular Pharmacology 69 (2006) 11–18.
[24] U. Pentikainen, L. Settimo, M.S. Johnson, O.T. Pentikainen, Subtype selectivity and flexibility of ionotropic glutamate receptors upon antagonist ligand binding, Organic and Biomolecular Chemistry 4 (2006) 1058–1070.
[25] A.Y. Lau, B. Roux, The free energy landscapes governing conformational changes in a glutamate receptor ligand-binding domain, Structure 15 (2007) 1203–1214.
[26] E.J. Bjerrum, P.C. Biggin, Rigid body essential X-ray crystallography: distinguishing the bend and twist of glutamate receptor ligand binding domains, Proteins 72 (2008) 434–446.
[27] K. Erreger, M.T. Geballe, S.M. Dravid, J.P. Snyder, D.J. Wyllie, S.F. Traynelis, Mechanism of partial agonism at NMDA receptors for a conformationally restricted glutamate analog, Journal of Neuroscience 25 (2005) 7858–7866.
[28] S.L. Kaye, M.S. Sansom, P.C. Biggin, Molecular dynamics simulations of the ligand-binding domain of an *N*-methyl-D-aspartate receptor, Journal of Biological Chemistry 281 (2006) 12736–12742.
[29] T. Yoshida, T. Seko, O. Okada, K. Iwata, L. Liu, K. Miki, M. Yohda, Roles of conserved basic amino acid residues and activation mechanism of the hyperthermophilic aspartate racemase at high temperature, Proteins 64 (2006) 502–512.
[30] Y. Tsfadia, R. Friedman, J. Kadmon, A. Selzer, E. Nachliel, M. Gutman, Molecular dynamics simulations of palmitate entry into the hydrophobic pocket of the fatty acid binding protein, FEBS Letters 581 (2007) 1243–1247.
[31] R.O. Drora, A.C. Pana, D.H. Arlowa, D.W. Borhania, P. Maragakisa, Y. Shana, H. Xua, D.E. Shaw, Pathway and mechanism of drug binding to G-protein-coupled receptors, PNAS 108 (2011) 13118–13123.
[32] K. Keinanen, W. Wisden, B. Sommer, P. Werner, A. Herb, T.A. Verdoorn, B. Sakmann, P.H. Seeburg, A family of AMPA-selective glutamate receptors, Science 249 (1990) 556–560.
[33] D.A. Case, T.A. Darden, T.E. Cheatham, III, C.L. Simmerling, J. Wang, R.E. Duke, R. Luo, K.M. Merz, D.A. Pearlman, M. Crowley, R.C. Walker, W. Zhang, B. Wang, S. Hayik, A. Roitberg, G. Seabra, K.F. Wong, F. Paesani, X. Wu, S. Brozell, V. Tsui, H. Gohlke, L. Yang, C. Tan, J. Mongan, V. Hornak, G. Cui, P. Beroza, D.H. Mathews, C. Schafmeister, W.S. Ross, P.A. Kollman, AMBER 9, University of California, San Francisco, 2006.
[34] P.A. Kollman, R. Dixon, W. Cornell, T. Fox, C. Chipot, A. Pohorille, The development/application of a 'minimalist' organic/biochemical molecular mechanics force field using a combination of ab initio calculations and experimental data, in: A. Wiljubsib, P. Weiner, W.F. van Gunsteren (Eds.), Computer Simulation of Biomolecular Systems, Vol. 3, Elsevier, 1997, pp. 83–96.
[35] W.L. Jorgensen, J. Chandrasekhar, J. Madura, M.L. Klein, Comparison of simple potential functions for simulation liquid water, Journal of Chemical Physics 79 (1983) 926–935.
[36] S. Izrailev, S. Stepaniants, M. Balsera, Y. Oono, K. Schulten, Molecular dynamics study of unbinding of the avidin–biotin complex, Biophysical Journal 72 (1997) 1568–1581.
[37] H. Lu, B. Isralewitz, A. Krammer, V. Vogel, K. Schulten, Unfolding of titin immunoglobulin domains by steered molecular dynamics simulation, Biophysical Journal 75 (1998) 662–671.
[38] G.M. Torrie, J.P. Valleau, Nonphysical sampling distributions in Monte Carlo free-energy estimation: umbrella sampling, Journal of Computational Physics 23 (1977) 187–199.
[39] T. Darden, D. York, L. Pedersen, Particle mesh Ewald: an *N*log(*N*) method for Ewald sums in large systems, Journal of Chemical Physics 98 (1993) 10089–10092.
[40] K. Odai, T. Sugimoto, M. Kubo, E. Ito, Theoretical research on structures of γ-aminobutyric acid and glutamic acid in aqueous conditions, Journal of Biochemistry 133 (2003) 335–342.
[41] J.P. Ryckaert, G. Ciccotti, H.J.C. Berendsen, Numerical integration of the Cartesian equations of motion of a system with constraints: molecular dynamics of n-alkanes, Journal of Computational Physics 23 (1977) 327–341.
[42] H.J.C. Berendsen, J.P.M. Postma, W.F. van Gunsteren, A. DiNola, J.R. Haak, Molecular dynamics with coupling to an external bath, Journal of Chemical Physics 81 (1984) 3684–3690.
[43] H.C. Andersen, Molecular dynamics simulations at constant pressure and/or temperature, Journal of Chemical Physics 72 (1980) 2384–2393.
[44] W. Humphrey, A. Dalke, K. Schulten, VMD — visual molecular dynamics, Journal of Molecular Graphics 14 (1996) 33–38.
[45] A. Noy, A. Pérez, C.A. Laughton, M. Orozco, Theoretical study of large conformational transitions in DNA: the B<—>A conformational change in water and ethanol/water, Nucleic Acids Research 35 (2007) 3330–3338.
[46] S. Kumer, D. Bouzida, R. Swendsen, P. Kollman, J. Rosenberg, The weighted histogram analysis method for free-energy calculations on biomolecules. I. The method, Journal of Computational Chemistry 13 (1992) 1011–1021.
[47] http://membrane.urmc.rochester.edu/Software/WHAM/WHAM.html.
[48] N. Go, A theorem on amplitudes of thermal atomic fluctuations in large molecules assuming specific conformations calculated by normal mode analysis, Biophysical Chemistry 35 (1990) 105–112.
[49] A. Kitao, F. Hirata, N. Go, The effects of solvent on the conformation and the collective motions of protein: normal mode analysis and molecular dynamics simulations of melittin in water and in vacuum, Chemical Physics 158 (1991) 447–472.
[50] B. Brooks, D. Janezic, M. Karplus, Harmonic analysis of large systems. I. Methodology, Journal of Computational Chemistry 16 (1995) 1522–1542.
[51] W. Wriggers, K. Schulten, Protein domain movements: detection of rigid domains and visualization of effective rotations in comparisons of atomic coordinates, Proteins 29 (1997) 1–14.
[52] K. Kinoshita, H. Nakamura, Identification of the ligand binding sites on the molecular surface of proteins, Protein Science 14 (2005) 711–718.
[53] T. Mamonova, K. Speranskiy, M. Kurnikova, Interplay between structural rigidity and electrostatic interactions in the ligand binding domain of GluR2, Proteins 73 (2008) 656–671.
[54] K. Sato, Y. Ito, T. Yomo, K. Kaneko, On the relation between fluctuation and response in biological system, Proceedings of the National Academy of Sciences of the United States of America 100 (2003) 14086–14090.
[55] M. Ikeguchi, J. Ueno, M. Sato, A. Kidera, Protein structural change upon ligand binding: linear response theory, Physical Review Letters 94 (078102) (2005) 1–4.
[56] J.P. Gallivan, D.A. Dougherty, Cation–π interactions in structural biology, Proceedings of the National Academy of Sciences of the United States of America 96 (1999) 9459–9464.
[57] S. Mecozzi, A.P. West Jr., D.A. Dougherty, Cation—π interactions in simple aromatics: electrostatics provide a predictive tool, Journal of the American Chemical Society 118 (1996) 2307–2308.
[58] R. Abele, K. Keinanen, D.R. Madden, Agonist-induced isomerization in a glutamate receptor ligand-binding domain, Journal of Biological Chemistry 275 (2000) 21355–21363.
[59] Q. Cheng, M. Du, G. Ramanoudjame, V. Jayaraman, Evolution of glutamate interactions during binding to a glutamate receptor, Nature Chemical Biology 1 (2005) 329–332.
[60] M.K. Fenwick, R.E. Oswald, On the Mechanisms of α-Amino-3-hydroxy- 5-methylisoxazole-4-propionic acid (AMPA) receptor binding to glutamate and kainite, Journal of Biological Chemistry 285 (2010) 12334–12343.
[61] T. Mamonova, M.J. Yonkunas, M.G. Kurnikova, Energetics of the cleft closing transition and the role of electrostatic interactions in conformational rearrangements of the glutamate receptor ligand binding domain, Biochemistry 47 (2008) 11077–11085.